Modelling tree roots in mixed forest stands by inhomogeneous marked Gibbs point processes

Stefanie Eckel[*1], **Frank Fleischer** [2], **Pavel Grabarnik** [3], **Marian Kazda** [4], **Aila Särkkä** [5], and **Volker Schmidt** [1]

[1] Ulm University, Institute of Stochastics, Helmholtzstr. 18, 89069 Ulm, Germany
[2] Boehringer Ingelheim Pharma GmbH & Co. KG, Medical Data Services/Biostatistics, Birkendorfer Straße 65, 88397 Biberach a. d. R., Germany
[3] Russian Academy of Sciences, Institute of Physico-Chemical and Biological Problems of Soil Science, 142290 Pushchino, Russia
[4] Ulm University, Institute of Systematic Botany and Ecology, Albert-Einstein-Allee 11, 89081 Ulm, Germany
[5] Chalmers, Department of Mathematical Statistics, and University of Gothenburg, Department of Mathematical Statistics, 41296 Gothenburg, Sweden

Summary

The aim of the paper is to apply point processes to root data modelling. We propose a new approach to parametric inference when the data are inhomogeneous replicated marked point patterns. We generalize Geyer's saturation point process to a model which combines inhomogeneity, marks and interaction between the marked points. Furthermore, the inhomogeneity influences the definition of the neighborhood of points. Using the maximum pseudolikelihood method, this model is then fitted to root data from mixed stands of Norway spruce (*Picea abies (L.) Karst.*) and European beech (*Fagus sylvatica L.*) to quantify the degree of root aggregation in such mixed stands. According to the analysis there is no evidence that the two root systems are not independent.

Key words: bivariate spatial point process, Geyer's saturation point process, inhomogeneity, interaction, replicated point patterns, root modelling.

1 Introduction

Statistical analysis and modelling of complex point patterns is a challenging topic in modern spatial statistics (Baddeley et al., 2006; Diggle, 2003; Finkenstädt, Held and Isham, 2006; Illian et al., 2008). For example, such point patterns arise by observing plant roots in soils. Typically, available data come from field experiments when one or several root systems are sectioned by a profile wall and root ends within the wall are mapped. The root data are characterized as inhomogeneous (mainly vertically), clustered and small sampled patterns. Each of these properties is a subject of intense research in recent time (see the references below). Obviously, a much more difficult task is given when these properties appear simultaneously for the point patterns under investigation.

Previous works on the root distribution in pure stands report that the vertical root intensity can be described as a one-dimensional depth function (Parker and van Lear, 1996; Schenk, 2005) with the greatest root density in the top soil layers for most forests (Jackson and Caldwell, 1996). Yet, it turned out that a vertical homogenization cannot eliminate clustering properties of root patterns. Therefore, some models for clustering should be applied to the data. For root patterns in pure stands inhomogeneous Matérn cluster point processes have been fitted (Fleischer et al., 2006) using a vertical homogenization based on the depth root density.

* Corresponding author: e-mail: stefanie.eckel@uni-ulm.de, Phone: +00 49 731 5031086, Fax: +00 49 731 5023649

However, this approach cannot be used for root data in mixed stands, since the vertical root distributions of different species may be different (Schmid and Kazda, 2001) and thus the homogenization step cannot be applied. Moreover, the Matérn cluster process does not allow to model interaction between roots of different species. Our approach to model interspecific interaction of roots in mixed stands is to use inhomogeneous marked Gibbs point processes which are able to represent both long-range inhomogeneity in the vertical direction as well as short-range variability of the intensity (clustering). The novelty of the present paper is the introduction and combination of several ingredients of an inhomogeneous marked Gibbs point process model. Let us describe them briefly.

Inhomogeneity. There exist several approaches to include inhomogeneity in Gibbs models. One of them is to allow a parameter controlling the intensity to depend on location (Baddeley and Turner, 2000; Ogata and Tanemura, 1986; Stoyan and Stoyan, 1998). This seems natural when the range of interaction does not vary from one location to another, being motion-invariant. Another approach suggested in Jensen and Nielson (2000) and Nielson and Jensen (2004) uses transformations of Gibbs point processes, where all interaction functions, including one-point interactions, are subject to local dependency that implies some anisotropy effect which may be undesirable in applications. A possible way to overcome this drawback is local scaling (Hahn et al., 2003) where two-points and higher order interaction functions depend on location. Our paper presents a different approach to accommodate inhomogeneity in Gibbs models. We allow the one-point interaction function controlling the intensity to vary in space as in the first class of models cited above, while the influence zones, a neighborhood relation, of roots are allowed to depend on the vertical variation of root density. We believe that the suggested way to model inhomogeneity is appropriate for this application, since the size of the interaction distance increases with depth, while the rest of the long-range inhomogeneity can be explained by a parameter responsible for changing the intensity of the point process.

Clustering. The class of pairwise interaction point processes, a special class of Gibbs point processes, is often used in applications (Diggle et al., 1994). However, such processes are suitable for modelling regularity but not clustering (Baddeley and van Lieshout, 1995; Grabarnik and Särkkä, 2001; Møller, 1999). Various ways to overcome this difficulty were proposed in the literature, e.g. area-interaction point processes (Baddeley and van Lieshout, 1995) and continuous random cluster Markov point processes (Møller, 1999). However, it is not clear how to generalize them to the multivariate case. Another class of Gibbs models capable to produce a variety of clustered patterns was proposed in Grabarnik and Särkkä (2001). These point processes are an extension of Geyer's saturation model (Geyer, 1999) and can be generalized to the marked or multivariate case. We choose the bivariate saturation point process model on the basis of the parsimonious principle. Here, only one parameter is needed to describe one type of interaction. Additional parameters which potentially control clustering can be chosen ad hoc, for example by some trial experiments.

Parameter estimation. The estimation of parameters is problematic for Gibbs models. Since a direct maximization of the likelihood is unfeasible, Monte Carlo approximation of the likelihood can be an appropriate solution (Geyer, 1999; Møller and Waagepetersen, 2004). A computationally easier alternative approach is the maximum pseudolikelihood method (Baddeley and Turner, 2000; Goulard, Särkkä and Grabarnik, 1996) which was taken here because it does not require heavy computations for the maximization. Although we do not use simulation for the estimation of parameters, a simulation algorithm based on Markov chain Monte Carlo (MCMC) methodology is presented in this work because it is used for checking the goodness-of-fit of the estimated model.

Replicated patterns. Frequently, methods of spatial statistics operate with data when only one single point pattern is available. Less attention has been paid to replicated data, i.e. several profile walls. An extension of the estimation method to replicated data is straightforward if we allow the parameters to vary across replicates and assume common values for interactions (Diggle, Mateu and Clough, 2000; Mateu, 2001). A more advanced technique based on generalized linear mixed modelling was proposed by Bell and Grundwald (2004), where the assumption of a common interaction parameter for all replicates can be relaxed.

Besides presenting a new approach to deal with the above mentioned challenges, our aim of the point process modelling of root data is to quantify the degree of root aggregation in mixed stands of Norway spruce (*Picea abies* (L.) Karst.) and European beech (*Fagus sylvatica* L.). Thus, we are going to model intraspecific and interspecific interactions between roots of different species. The study of root patterns provide information which allows us to better understand subsurface processes in tree stands and how roots exploit soil resources. A further advantage of the stochastic modelling of roots is that it can be used for the improved estimation of root biomass by a root-wall intersection counting (Grabarnik, Loic and Bengough, 1998).

Note that roots are actually fibres in 3D, but we consider points in 2D. Krasnoperov and Stoyan (2004) showed that for stationary and isotropic fibre processes the pair correlation function of the 2D point process of the (centre) points of the fibre sectioning profiles can be used as the estimator for the reduced pair correlation function of the 3D fibre process. The reduced pair correlation function refers to the case where only the fibre point pairs from two different fibres are included. We can assume isotropy of the root fibre processes but not stationarity. However, after the transformations, we have first-order stationarity with respect to each species. Therefore, the univariate 2D second-order properties based on the transformed point patterns on the profiles can be used to gain information about the 3D second-order properties of the root system. Thus, for example, if the 2D second-order properties indicate the absence of interaction, then there is no evidence that the roots themselves interact in 3D.

Stereological methods of an analysis of gradient structures which in fact are relevant to our experimental situation were studied in Hahn et al. (1999). Their approach was model-based using gradient Boolean and gradient Poisson-Voronoi tessellation models. In the Boolean model diameters of spherical grains were location-dependent.

The paper is organized as follows. In Section 2 we briefly describe the data, i.e. the acquisition of the profile walls of roots of the two tree species, *P. abies* and *F. sylvatica*. In Section 3 we introduce a generalized version of Geyer's saturation point process which combines inhomogeneity, locally dependent neighbor relation and interaction between the marked points. The model fitting of this generalized model to replicated point patterns is described in Section 4. Furthermore, Section 5 proposes a simulation algorithm for this generalized model. In Section 6 we present the results of the model fitting to root data in mixed stands of *P. abies* and *F. sylvatica*. Finally, in Section 7 we give a short discussion of the presented method and the obtained results.

2 Data description

For details of site description, pit excavation, root mapping and previous results, see Fleischer et al. (2006) and Schmid and Kazda (2001, 2002, 2005). Investigations in the present paper are based upon these articles and thus only a short summary of the most important facts regarding the root data is given here.

Data collection took place near Wilhelmsburg, Austria (4805'51" N, 1539'48" E) in mixed stands of *P. abies* and *F. sylvatica* located between pure stands of both species. One experimental plot of about 0.5 ha was selected within each stand. The area was situated at an altitude of 480 m, an aspect of NNE and an inclination of 10%. The tree population was 55 years old, the dominant tree height was 28 m and the stand densities of *P. abies* and *F. sylvatica* (16.1 and 26.1 m^2/ha) were similar to each other. The soils with only thin organic layer (about 4 cm) can be classified as stagnic cambisols developed from Flysch sediments. Annual rainfall in Wilhelmsburg averages 843 mm with a mean summer precipitation from May to September being 433 mm. The mean annual temperature is $8.4°C$, and the mean summer temperature is $15.7°C$.

In these stands 20 soil pits were excavated, leading to 7 vertical profile walls that are analyzed in the following. The other profile walls could not be used due to extreme unequal numbers of roots of *F. sylvatica* and *P. abies*. On each wall all coarse roots were identified and divided into living and dead. All living small roots (25 mm) were marked with pins and digitally photographed. These pictures were evaluated and a

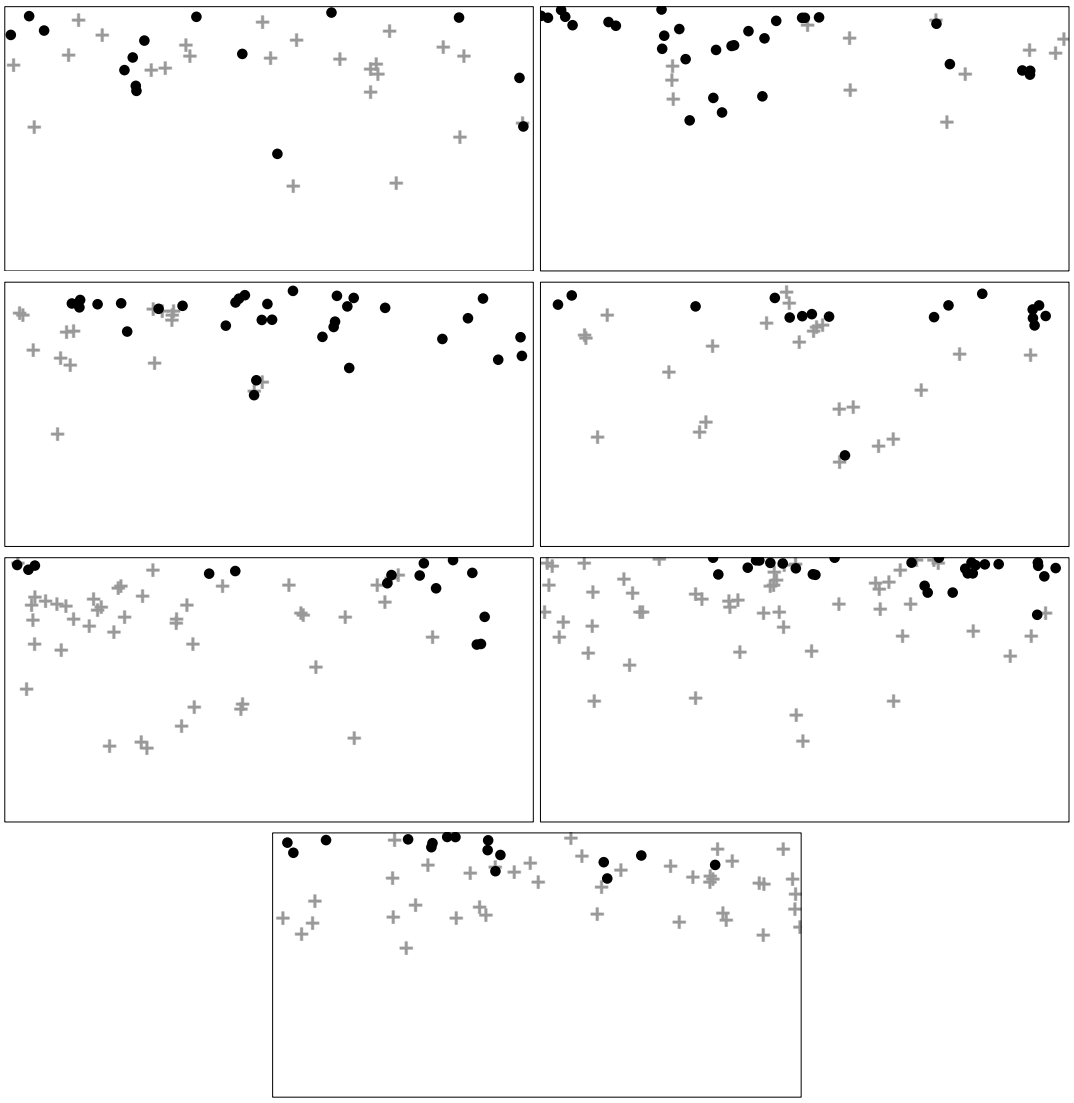

Fig. 1 Original bivariate point patterns from mixed stands of *P. abies* (•) and *F. sylvatica* (+)

coordinate plane was drawn over each profile wall, so that every root corresponds to a (marked) point in the plane. After the root mapping, the ends of roots within the profile walls are regarded as realizations of a stochastic planar bivariate point process observed within the sampling window W with area $|W|$ = 200 cm (width) $\times$ 100 cm (height) (Fig. 1).

It was shown in Schmid and Kazda (2001) that the vertical root distributions of *P. abies* and *F. sylvatica* in these mixed stands can be approximated by an exponential and a Gamma distribution, respectively (see also Section 3 in this paper). The fitted parameters of these distributions are $\widehat{\eta} = 11.92$ for *P. abies* and $\widehat{\alpha} = 2.382$, $\widehat{\beta} = 10.81$ for *F. sylvatica*.

Note that the number of points in each profile wall is rather small, but the only possibility to enlarge the sampling window would be with respect to the horizontal direction (there are no roots above and below our current sampling windows). The problem which would arise then is the horizontal inhomogeneity, i.e. the profile wall would range too close to a beech tree or spruce tree, respectively, such that the number

of detected roots and the interactions between the roots would then be influenced by non-equal sampling conditions. Therefore, the only way to increase the data set in this experiment is to increase the number of replications.

3 Model description

One could try to model the bivariate point pattern of root locations by two independent Matérn cluster point processes, one for *P. abies* and one for *F. sylvatica*. However, then we would lose from the very beginning the possible interaction between the two species. We have decided to model the root locations by Gibbs point processes, which are often used as models for point patterns with interactions.

Since our root data is clustered (Schmid and Kazda, 2005), the simplest interaction model, the Strauss process (Strauss, 1975), is not applicable (Møller, 1999). We believe that using instead Geyer's saturation point process (Geyer, 1999) would be a good choice on a parsimonious basis. Grabarnik and Särkkä (2001) extended the saturation process introducing models with a more general interaction structure. In the present paper we generalize Geyer's model to the bivariate case and include inhomogeneity in the model.

A bivariate point process can be considered as a marked point process $X = \{(X_n; m(X_n))\}$ where marks m attached to every point of the point process are binary variables $m \in \{1, 2\}$ and therefore, the process X consists of two components $X^{(1)} = \{(X_k; 1)\}$ and $X^{(2)} = \{(X_j; 2)\}$. Note that in the following, we will write $x^{(i)}$ instead of $(x; i)$ for a point x of type i for easier reading of some formulae below. In our case we specify that mark 1 refers to *P. abies* and mark 2 to *F. sylvatica*. It is characteristic for marked Gibbs point processes that they are defined by a density function f with respect to the distribution of the homogeneous independently marked Poisson reference process with intensity 1 on W (Goulard et al., 1996; Møller and Waagepetersen, 2004).

3.1 Bivariate inhomogeneous saturation point process

Let us foremost recall the saturation point process introduced by Geyer (1999) to replace the Strauss process for clustered data. Let us preliminarily ignore the marks, and give the original definition of the process. A (non-marked) point process X is called a saturation process if the density function f (with respect to the Poisson reference process of unit intensity) has the form

$$f(\mathbf{x}) = ab^n \prod_{x \in \mathbf{x}} \gamma^{\min\{d, N_{\mathbf{x}}(x)\}},$$

where $\mathbf{x} \subset \mathbb{R}^2$ denotes any finite point configuration, $a > 0$ is a normalizing constant, b controls the intensity of the point process X, n is the number of elements of the set $\mathbf{x}$, γ is the interaction parameter, d is the saturation threshold (an upper bound on the contribution to the density f of any single point), and $N_{\mathbf{x}}(x)$ is the number of neighbors in $\mathbf{x}$ of the point $x \in \mathbf{x}$. In the original model, two points are said to be neighbors if they are closer to each other than some fixed distance. Furthermore, $\gamma < 1$ indicates repulsion, $\gamma > 1$ clustering, and $\gamma = 1$ the Poisson case.

However, we have two types of roots and some inhomogeneity in the point patterns and therefore, we define a bivariate inhomogeneous version of the above saturation point process. A marked point process X in $W \subset \mathbb{R}^2$ with mark space $\{1, 2\}$ is called a bivariate inhomogeneous saturation point process if its density f (with respect to the bivariate unit rate Poisson reference process with independent marks) has the form

$$\begin{aligned} f(\mathbf{x}) \quad = \quad & ab_1^{n_1} b_2^{n_2} \prod_{x \in \mathbf{x}^{(1)}} b_1'(x) \gamma_1^{\min\{d_1, N_{1,\mathbf{x}^{(1)}}(x)\}} \gamma_{12}^{\min\{d_{12}, N_{1,\mathbf{x}^{(2)}}(x)\}} \\ & \prod_{x \in \mathbf{x}^{(2)}} b_2'(x) \gamma_2^{\min\{d_2, N_{2,\mathbf{x}^{(2)}}(x)\}} \gamma_{12}^{\min\{d_{12}, N_{2,\mathbf{x}^{(1)}}(x)\}}, \end{aligned} \tag{1}$$

where $\mathbf{x} = \{\mathbf{x}^{(1)}, \mathbf{x}^{(2)}\}$ with $\mathbf{x}^{(i)} = \{x_1^{(i)}, \ldots, x_{n_i}^{(i)}\}$. Furthermore, $a > 0$ is the normalizing constant, b_i controls the intensity of the process $X^{(i)}$, $b_i'(x)$ is the depth density function at location x of $X^{(i)}$, and n_i is the number of points of $\mathbf{x}^{(i)}$ in W. The within-species interaction parameter for type i is γ_i, and d_i is the saturation threshold of $X^{(i)}$ (upper bound on the number of neighbors). The parameter γ_{12} describes the inter-species interaction, and d_{12} is the upper bound on the number of neighbors of different type counted for a given point. Finally, $N_{i,\mathbf{x}^{(j)}}(x)$ is the number of points of $\mathbf{x}^{(j)}$ in the neighborhood of a point x of type i, and $j \neq i$.

Note that the density f of a homogeneous version of the bivariate saturation process has the same form as in (1) but without the terms $b_i'(x)$, $i = 1, 2$. Furthermore, the inter-species interaction parameter γ_{12} equals 1 if the two patterns are independent.

3.2 Modelling of inhomogeneity

We define that two points $x \in \mathbf{x}^{(i)}$ and $y \in \mathbf{x}^{(j)}$, $i, j = 1, 2$, are neighbors if their influence regions overlap. For the definition of the influence region, we use the following approach: We take circles with interaction radius r_i ($i = 1, 2$) and transform them vertically according to the exponential and Gamma distribution, which results in quasi ellipsoidal influence regions (Fig. 2). More precisely, the influence region $I_i(x)$ of a point $x = (w, h)$, where w is the horizontal and h is the vertical coordinate, respectively, of type i is given by

$$I_i(x) = \{(u, v) : (u - w)^2 + h_W[F_i(v) - F_i(h)]^2 \leq r_i^2\},$$

where F_i denotes the depth distribution function for type i, i.e.

$$F_1(h) = 1 - e^{-\frac{1}{\eta}h}$$

and

$$F_2(h) = \int_0^h \frac{1}{\Gamma(\alpha)\beta^\alpha} s^{\alpha-1} e^{\frac{-s}{\beta}} ds,$$

$h_W = 100\,cm$ denotes the height of the sampling window and the parameters η, α and β are given in Section 2. The reason for choosing such influence regions is that the expected number of neighbor points would then be equal in each depth.

Making a homogenization by a transformation of the influence zones we do not take out all inhomogeneity occurring in the data. Further variability in space can be controlled by allowing the intensity parameters of our model to depend on location.

Recall that in our model additional parameters $b_i'(x)$ controlling the intensities of points are used to model the inhomogeneity with respect to the vertical axis. These functions are assumed to have the following forms:

$$b_1'(w, h) = \frac{1}{\eta'} e^{-\frac{1}{\eta'}h}$$

and

$$b_2'(w, h) = \frac{h^{\alpha'-1} e^{-\frac{h}{\beta'}}}{\Gamma(\alpha')\beta'^{\alpha'}}$$

for *P. abies* and *F. sylvatica*, respectively, where $\eta', \alpha', \beta' > 0$ are some parameters.

There are different possibilities to choose the parametric form of the $b_i'(x)$ functions, i.e. different functions may be used for different root systems. Note that *P. abies* has a sinker root system and *F. sylvatica* possesses a heart root system. We chose the exponential and Gamma distributions, respectively, since the same shape differences are still present in the inhomogeneity functions $b_i'(x)$ after the homogenization of the influence zones.

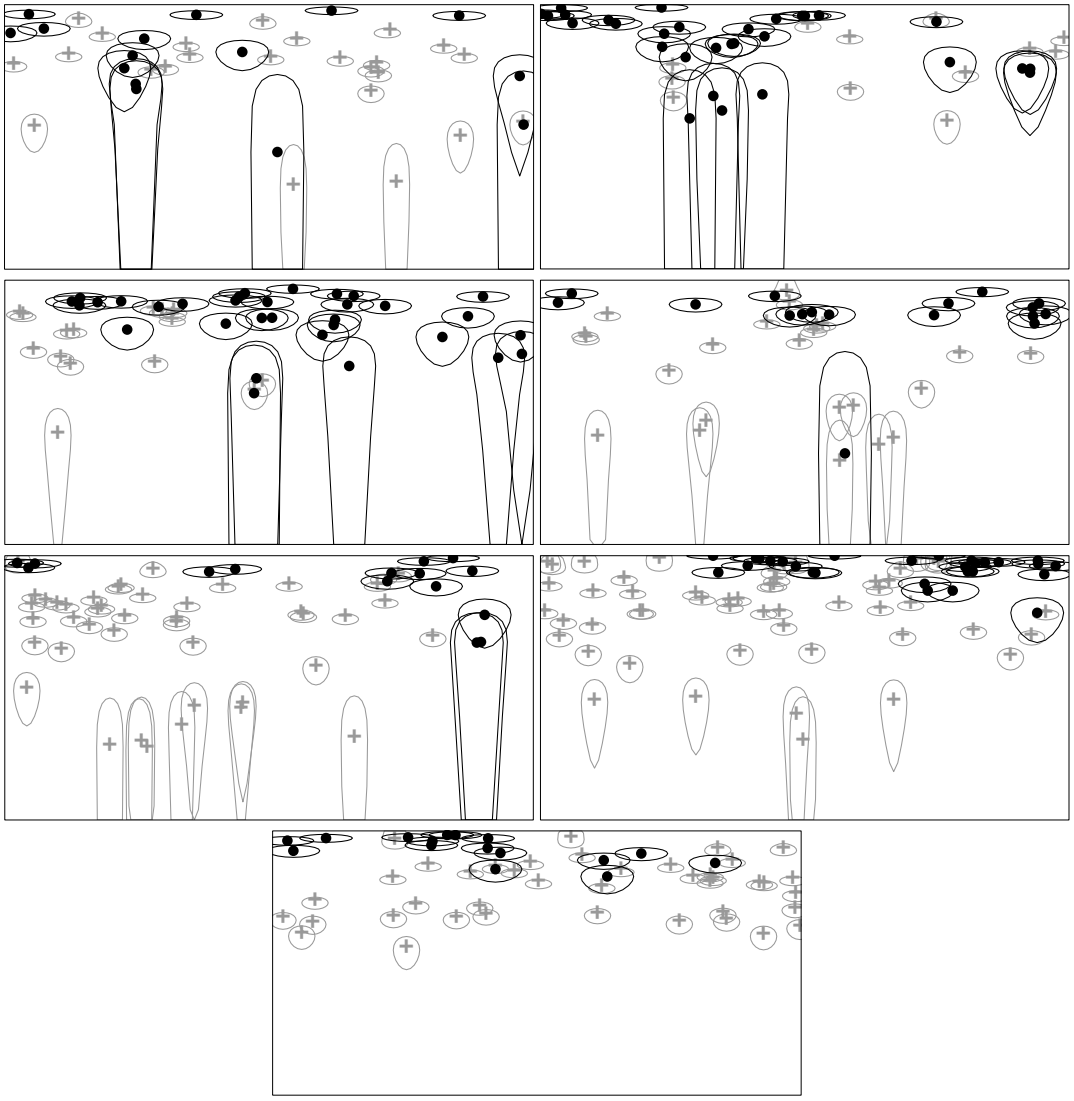

Fig. 2 Influence regions for *P. abies* (•) and *F. sylvatica* (+)

It is necessary to stress that if there is no interaction between points, i.e. all γ are equal to 1, the estimated parametric functions $b_i'(x)$ in the model coincide with the intensity functions normalized by the overall intensities. In contrast, the interactions between the roots (or points in the data) affect the estimated inhomogeneity parameters and thus estimates of η', α' and β' can differ from the values of the parameters η, α and β of the depth distributions which are used in the modelling of the influence zones.

To show this effect we made several simulation experiments with a non-marked version of the inhomogeneous saturation model introduced in (1). The results thereof are visualized in Fig. 3. For simplicity we considered only the exponential distribution with $\eta' = 0.2$ in a sampling window $W = 1 \times 1$ with circular influence regions ($r_1 = 0.02$) and a saturation threshold $d_1 = 4$. It is obvious that if the interaction parameter changes, then the intensity of points changes as well. A similar observation was made in Stoyan and Stoyan (1998) for inhomogeneous hard core point processes.

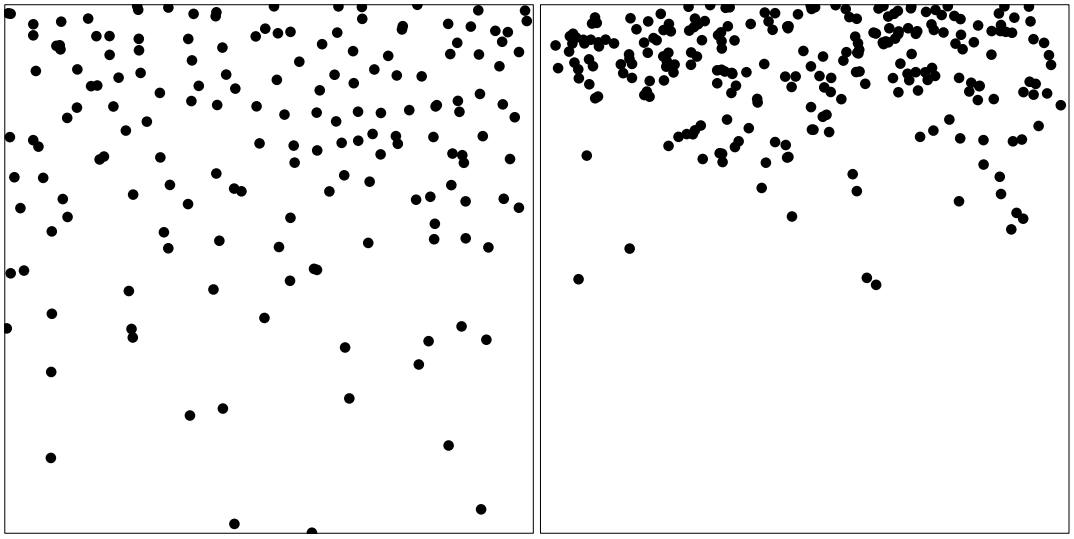

(a) $\gamma_1 = 0.6, b_1 = 500, \eta' = 0.2$ (b) $\gamma_1 = 1.4, b_1 = 70, \eta' = 0.2$

Fig. 3 Realizations of (non-marked) inhomogeneous saturation point processes for which inhomogeneity terms are equal

3.3 Conditional intensity

In order to simulate the point process and to estimate the model parameters, the conditional intensities $\lambda_i(u, \mathbf{x})$ are needed. They are defined as a ratio of density functions and heuristically, they tell us how likely it is to have a point at location u with mark i given that the rest of the marked point pattern coincides with $\mathbf{x}$. The conditional intensities $\lambda_i(u, \mathbf{x})$ depend only on the marked point $u^{(i)}$ and its neighbors in $\mathbf{x}$ and do not include any normalizing constant.

The conditional intensity $\lambda(u, \mathbf{x})$ for the (non-marked) Geyer point process for $u \notin \mathbf{x}$ is given by (Geyer, 1999)

$$\lambda(u, \mathbf{x}) = b\gamma^{\min\{d, N_{\mathbf{x}}(u)\}} \prod_{x \in \mathbf{x}}^{n} \gamma^{\min\{d, N_{\mathbf{x}\cup\{u\}}(x)\} - \min\{d, N_{\mathbf{x}}(x)\}}.$$

For the bivariate inhomogeneous saturation point process, the conditional intensities are given by

$$\lambda_i(u, \mathbf{x}) = \frac{f(\mathbf{x} \cup \{u^{(i)}\})}{f(\mathbf{x})} = b_i b_i'(u) \gamma_i^{\min\{d_i, N_{i,\mathbf{x}^{(i)}}(u)\} + \sum_{x \in \mathbf{x}^{(i)}} \delta_{i,u}(x)} \gamma_{12}^{\min\{d_{12}, N_{i,\mathbf{x}^{(j)}}(u)\} + \sum_{x \in \mathbf{x}^{(j)}} \delta_{ji,u}(x)},$$

if $u \notin \mathbf{x}^{(i)}$, where $\mathbf{x} = \{\mathbf{x}^{(1)}, \mathbf{x}^{(2)}\}$,

$$\mathbf{x} \cup \{u^{(i)}\} = \begin{cases} \{\mathbf{x}^{(1)} \cup \{u\}, \mathbf{x}^{(2)}\} & \text{if } i = 1, \\ \{\mathbf{x}^{(1)}, \mathbf{x}^{(2)} \cup \{u\}\} & \text{if } i = 2, \end{cases}$$

$$\delta_{i,u}(x) = \begin{cases} 1 & \text{if } N_{i,\mathbf{x}^{(i)}}(x) < N_{i,\mathbf{x}^{(i)}\cup\{u\}}(x) \leq d_i, \\ 0 & \text{otherwise,} \end{cases}$$

and

$$\delta_{ji,u}(x) = \begin{cases} 1 & \text{if } N_{j,\mathbf{x}^{(i)}}(x) < N_{j,\mathbf{x}^{(i)}\cup\{u\}}(x) \leq d_{12}, \\ 0 & \text{otherwise.} \end{cases}$$

In case of $u \in \mathbf{x}^{(i)}$ the formulae for $\lambda_i(u,\mathbf{x})$, $\delta_{i,u}(x)$ and $\delta_{ji,u}(x)$ are modified as

$$\begin{aligned}\lambda_i(u,\mathbf{x}) &= \frac{f(\mathbf{x})}{f(\mathbf{x}\setminus\{u^{(i)}\})} \\ &= b_i b_i'(u)\gamma_i^{\min\{d_i, N_{i,\mathbf{x}^{(i)}\setminus\{u\}}(u)\}+\sum_{x\in\mathbf{x}^{(i)}\setminus\{u\}}\delta_{i,u}(x)}\gamma_{12}^{\min\{d_{12},N_{i,\mathbf{x}^{(j)}}(u)\}+\sum_{x\in\mathbf{x}^{(j)}}\delta_{ji,u}(x)},\end{aligned}$$

$$\delta_{i,u}(x) = \begin{cases} 1 & \text{if } N_{i,\mathbf{x}^{(i)}\setminus\{u\}}(x) < N_{i,\mathbf{x}^{(i)}}(x) \le d_i, \\ 0 & \text{otherwise,}\end{cases}$$

and

$$\delta_{ji,u}(x) = \begin{cases} 1 & \text{if } N_{j,\mathbf{x}^{(i)}\setminus\{u\}}(x) < N_{j,\mathbf{x}^{(i)}}(x) \le d_{12}, \\ 0 & \text{otherwise.}\end{cases}$$

4 Model fitting

For the estimation of model parameters it is assumed that the density $f(\mathbf{x};\theta)$ is known up to some parameter vector $\theta = (\theta_1, ..., \theta_p)$. To estimate θ, we have chosen to use the pseudolikelihood method (Baddeley and Turner, 2000; Goulard et al., 1996). Only the conditional intensities $\lambda_i(x,\mathbf{x};\theta)$ which do not depend on the unknown normalizing constant are needed in order to write down (and maximize) the pseudolikelihood function and therefore, the method is computationally convenient. Also, it is known how to estimate the overall parameters from replicated point patterns by this method.

4.1 Pseudolikelihood method

The pseudolikelihood function of a marked point process with two marks is given by (Goulard et al., 1996)

$$\mathrm{PL}(\theta;\mathbf{x}) = \prod_{x\in\mathbf{x}^{(1)}} \lambda_1(x,\mathbf{x})\exp(-\int_W \lambda_1(u,\mathbf{x})du) \prod_{x\in\mathbf{x}^{(2)}} \lambda_2(x,\mathbf{x})\exp(-\int_W \lambda_2(u,\mathbf{x})du),$$

where the conditional intensities $\lambda_i(x,\mathbf{x}) = \lambda_i(x,\mathbf{x};\theta)$ depend on the unknown parameter vector θ.

Substituting the conditional intensities for the bivariate inhomogeneous saturation point process and taking the logarithm, we obtain the log pseudolikelihood function which is used for the estimation of model parameters:

$$\begin{aligned}\log\ \mathrm{PL}(\theta;\mathbf{x}) &= n_1\log b_1 + \sum_{x\in\mathbf{x}^{(1)}}\log b_1'(x) + n_2\log b_2 + \sum_{x\in\mathbf{x}^{(2)}}\log b_2'(x) \\ &\quad + \log\gamma_1\left(\sum_{x\in\mathbf{x}^{(1)}}[\min\{d_1, N_{1,\mathbf{x}^{(1)}}(x)\} + \sum_{y\in\mathbf{x}^{(1)}\setminus\{x\}}\delta_{1,x}(y)]\right) \\ &\quad + \log\gamma_2\left(\sum_{x\in\mathbf{x}^{(2)}}[\min\{d_2, N_{2,\mathbf{x}^{(2)}}(x)\} + \sum_{y\in\mathbf{x}^{(2)}\setminus\{x\}}\delta_{2,x}(y)]\right) \\ &\quad + \log\gamma_{12}\left(\sum_{x\in\mathbf{x}^{(1)}}\min\{d_{12}, N_{1,\mathbf{x}^{(2)}}(x)\} + \sum_{x\in\mathbf{x}^{(1)}}\sum_{y\in\mathbf{x}^{(2)}}\delta_{21,x}(y)\right) \\ &\quad + \log\gamma_{12}\left(\sum_{x\in\mathbf{x}^{(2)}}\min\{d_{12}, N_{2,\mathbf{x}^{(1)}}(x)\} + \sum_{x\in\mathbf{x}^{(2)}}\sum_{y\in\mathbf{x}^{(1)}}\delta_{12,x}(y)\right) \\ &\quad - \sum_{s=1}^{k}\lambda_1(z_s^{(1)},\mathbf{x})w_s^{(1)} - \sum_{s=1}^{k}\lambda_2(z_s^{(2)},\mathbf{x})w_s^{(2)},\end{aligned}$$

where the two sums $\sum_{s=1}^{k} \lambda_1(z_s^{(1)}, \mathbf{x}) w_s^{(1)}$ and $\sum_{s=1}^{k} \lambda_2(z_s^{(2)}, \mathbf{x}) w_s^{(2)}$ are approximations of the integrals $\int_W \lambda_1(u, \mathbf{x}) du$ and $\int_W \lambda_2(u, \mathbf{x}) du$, respectively. The dummy points $z_1^{(i)}, ..., z_k^{(i)}$, $k = 25^2$, $i = 1, 2$, together with the data points $x^{(i)} \in X$ induce a Voronoi tessellation of W and $w_s^{(i)}$ is the weight of the dummy point $z_s^{(i)}$, i.e. the area of the Voronoi cell with nucleus $z_s^{(i)}$. This method has been proposed by Berman and Turner (1992) for far fewer data and dummy points which saves CPU time and provides the same results as quadrature rules. Here, the dummy points lie on an equidistant grid and the y-coordinate is transformed according to the density function defining the influence regions, since most of the points are located in the upper part of the sampling window. The estimates of the parameters $b_1, b_2, \gamma_1, \gamma_2, \gamma_{12}, \eta, \alpha$ and β are obtained by maximizing this log pseudolikelihood function with respect to them.

4.2 Replicated point patterns

Unlike point patterns which are typically analyzed by methods of spatial statistics, root data are seldom sufficiently large. A way to get more data is to sample independently several patterns and combine so-called replicated point patterns in one data set.

Extending the estimation method developed for a single point pattern to the replicated case is straightforward (Diggle et al., 2000). Under the assumption that the k point patterns are realizations of independent and identically distributed point processes we can construct a pooled pseudolikelihood

$$\log \ \mathrm{PL}(\theta; \mathbf{x_1}, ..., \mathbf{x_k}) = \sum_{s=1}^{k} \log \mathrm{PL}_s(\theta; \mathbf{x}_s),$$

where $\mathrm{PL}_s, s = 1, ..., k$ is the pseudolikelihood of the s^{th} replication. Maximization of $\log \mathrm{PL}(\theta; \mathbf{x_1}, ..., \mathbf{x_k})$ with respect to θ yields the estimates of the unknown parameters.

The assumption that the unknown parameters are identical for all replications can be relaxed. One way to do this is to condition on the number of points in each replicated point pattern (Diggle et al., 2000). An approach based on generalized linear mixed models is given in Bell and Grunwald (2004), where the use of models with random effects allows us to relax an assumption on a common interaction parameter.

4.3 Correction of edge effects

Because of the small numbers of roots, we have chosen to use periodic boundary conditions (Ripley, 1977) for edge correction. In our case this means that the sampling window W is wrapped onto a cylinder by identifying the opposite sides of W which are parallel to the y-axis, so that points at these two opposite edges of the sampling window may be considered neighbors. There are no roots above or below the sampling window, and therefore no edge correction parallel to the x-axis is needed.

4.4 A priori chosen parameters

The parameters which have to be specified a priori for the estimation procedure were obtained from further data analyses as well as from biological reasoning:

- For the radius of the influence regions we homogenized the data with respect to the vertical axis (Fleischer et al., 2006) and estimated the mean univariate pair correlation functions for both tree species (Fig. 4). The interaction radius seems to be around 20 cm and 10 cm, and thus we chose $r_1 = 10\ cm$ and $r_2 = 5\ cm$ as influence ranges for *P. abies* and *F. sylvatica*, respectively. The homogenization has been done separately for *P. abies* and *F. sylvatica* with $\widehat{\eta}$, $\widehat{\alpha}$ and $\widehat{\beta}$ from Section 2.

- The saturation thresholds were set to $d_1 = d_2 = d_{12} = 4$, since we believe that more than 4 neighbors seem to have no larger influence than just 4 neighbors.

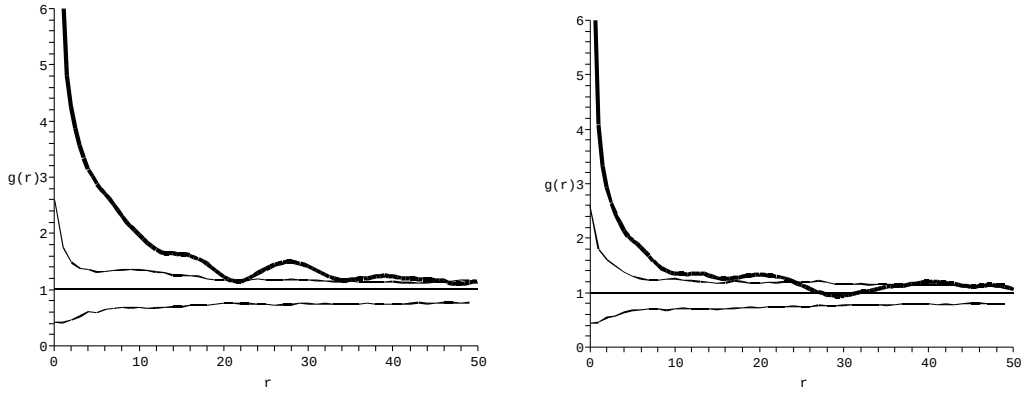

Fig. 4 Estimated mean univariate pair correlation functions $g(r)$ for homogenized data of *P. abies* (left) and *F. sylvatica* (right) with pointwise 99% envelopes (shown by thin lines) of CSR

5 Simulation

Although we do not use simulations for the estimation of the parameter vector θ, a simulation algorithm is presented. It is needed in this study for the goodness-of-fit testing. As it is the case for Gibbs point processes, a direct sampling is not feasible because of the intractability of the normalizing factor. A way to overcome this problem is to use a MCMC algorithm (Robert and Casella, 2004). We simulate the bivariate saturation point process by means of the Metropolis-Hastings algorithm (Møller and Waagepetersen, 2004), which allows us to simulate a Gibbs point process with either random or a fixed number of points. In the latter case updates are realized by shifting single points, whereas in the former case updates are performed by deaths, births and (optional) shifts. We use an algorithm where the updates can only be births or deaths of points. We chose a probability for the birth proposal as $p = 0.5$. The starting point configuration was the empty set. The number of iterations was set to 10000. The algorithm can be described as follows:

Step 1: Decide which mark will be considered
Choose mark i to be 1 with probability 0.5 and 2 otherwise.
Step 2: Update the point configuration **x** by a birth or a death
Propose a birth with probability p, i.e. generate a new point $q^{(i)}$ with mark i in W and accept $q^{(i)}$ with probability $\min\{\lambda_i(q, \mathbf{x})\frac{1-p}{p}\frac{|W|}{n_i+1}, 1\}$, otherwise propose a death, i.e. pick randomly a point $s^{(i)}$ of $\mathbf{x}^{(i)}$ and remove $s^{(i)}$ from **x** with probability $\min\{\lambda_i^{-1}(s, \mathbf{x})\frac{p}{1-p}\frac{n_i}{|W|}, 1\}$.
Step 3: Repeat steps 1 and 2 altogether 10000 times and take the resulting point configuration $\mathbf{x}$ as a final realization.

6 Results

Data analysis was done by using the GeoStoch library. Note that GeoStoch is a Java-based library system developed by the Institute of Applied Information Processing and the Institute of Stochastics at Ulm University which can be used for stochastic-geometric data analysis and spatial statistics (Mayer, Schmidt and Schweiggert, 2004). See also the internet description of this project under *http://www.geostoch.de*. For the maximization of the pseudolikelihood (see Section 4), existing software (R, 2006) for non-linear optimization has been used.

Homogeneity of replicated samples. To show that it is reasonable to assume that point patterns of the various profile walls are sampled from the same distribution, we plotted the individually estimated

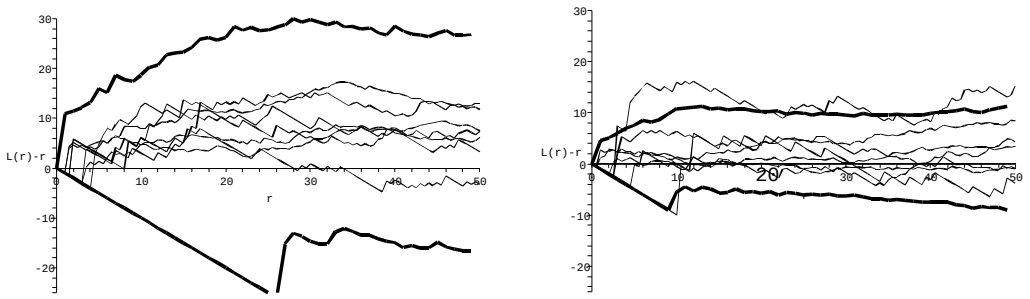

Fig. 5 Estimated $L(r) - r$ functions of each of the 7 profile walls for homogenized data of *P. abies* (left) and *F. sylvatica* (right) with pointwise 99% envelopes (shown by thick lines) of the fitted model

$L_{ii}(r) - r$ functions for the homogenized data in Fig. 5. Furthermore, we computed pointwise 99% envelopes for the $L(r) - r$ function based on 2000 simulation runs of the fitted model using only one replication. The estimated functions show the same statistical behaviour and run inside the envelopes, except for two curves of *F. sylvatica*. The curve which clearly runs outside the envelopes in Fig. 5 is estimated from the second profile wall on the left side in Fig. 1, where the number of roots of *F. sylvatica* is low and hence, variability of the estimate of the L-function is high. Thus, the model seems to be appropriate for each individual profile wall. From a biological point of view the assumption of an independent and identically distributed sample seems to be legitimate because the profile walls were dug each at a different place, where the surrounding (biological) conditions seem to have been similar (see Section 2).

Second-order statistics. Fig. 4 shows the estimated mean univariate pair correlation functions of the homogenized data which have already been used to obtain values for the interaction radii. The pointwise 99% envelopes for CSR are calculated by simulating the homogeneous Poisson point process 7 times in W (using 7 different estimated intensities) and estimating the replicated g_{ii}-functions for this simulation run. From 200 simulation runs we then compute the pointwise envelopes. Since the estimated functions are above the corresponding CSR envelopes, both species seem to have clustered root patterns. Thus, there is some indication that the parameters γ_1 and γ_2 cannot be eliminated from our model. Note that the pair correlation function is usually used for exploratory analysis of data while Ripley's K- (or L-) function is used for testing but here we use the pair correlation function for both purposes.

Estimates of parameters. The estimated values of the parameters $b_1, b_2, \gamma_1, \gamma_2, \gamma_{12}, \eta', \alpha'$ and β' for each individual point pattern are unstable, since there are too few points in each sampling window. But using the method described in Section 4.2 for replicated spatial point patterns, we obtain the following estimates:

- The parameters for the depth distributions of the roots of *P. abies* and *F. sylvatica* are estimated as $\widehat{\eta'} = 10.515$, $\widehat{\alpha'} = 2.0246$ and $\widehat{\beta'} = 12.323$, respectively.
- The parameters b_1, b_2 which control the intensities are estimated as $\widehat{b_1} = 0.0524$ and $\widehat{b_2} = 0.1194$ for *P. abies* and *F. sylvatica*, respectively.
- The interaction parameters γ_1, γ_2 and γ_{12} are estimated as $\widehat{\gamma_1} = 1.3294$ and $\widehat{\gamma_2} = 1.3165$ for *P. abies* and *F. sylvatica*, respectively and $\widehat{\gamma_{12}} = 0.9445$.

Note that changing the interaction radii and the saturation thresholds alters slightly the obtained values of the parameters, but the qualitative interpretation remains the same.

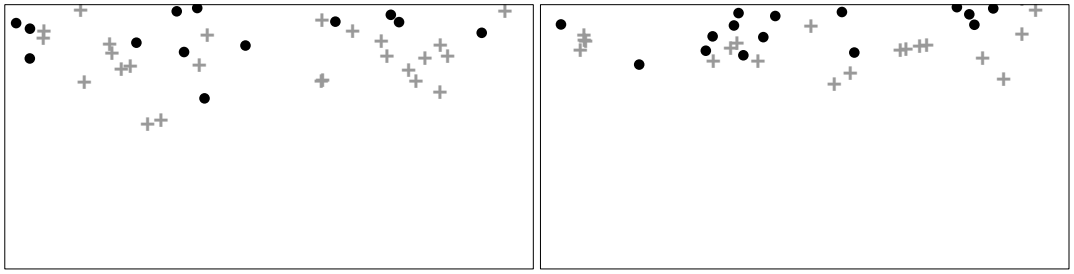

Fig. 6 Realizations of the estimated bivariate inhomogeneous saturation point process (*P. abies* •, *F. sylvatica* +)

	data	7 replications	14 replications
$\widehat{b_1}$	0.0524	0.0498 ± 0.0098	0.0483 ± 0.0057
$\widehat{b_2}$	0.1194	0.1144 ± 0.0141	0.1097 ± 0.0065
$\widehat{\gamma_1}$	1.3294	1.2907 ± 0.0907	1.2974 ± 0.0411
$\widehat{\gamma_2}$	1.3165	1.3250 ± 0.0761	1.3416 ± 0.0486
$\widehat{\gamma_{12}}$	0.9445	0.9250 ± 0.0525	0.9476 ± 0.0264
$\widehat{\eta'}$	10.515	10.127 ± 0.823	10.142 ± 0.480
$\widehat{\alpha'}$	2.0246	2.0079 ± 0.3163	2.0883 ± 0.2214
$\widehat{\beta'}$	12.323	12.869 ± 2.202	12.074 ± 1.304

Table 1 Mean values and standard deviations of the parameter estimates based on 50 simulations of 7 (middle) and 14 (right) replicates together with the values estimated from the data (left)

Fig. 6 shows two typical realizations of the bivariate inhomogeneous saturation point process obtained by the Metropolis-Hastings algorithm described in Section 5 using the parameters mentioned in the present section and in Section 4.4.

Accuracy of the estimates. In order to investigate the accuracy of the estimates, we simulated 50 realizations of our fitted model with 7 and 14 replications, respectively, and fitted the model to the simulated replicated data. The mean and standard deviations of the estimated parameters are presented in Tab. 1. It can be seen that the estimates obtained are reliable enough when using replicates (as in the experiment) to enlarge the data set, and doubling the number of replications, i.e. doubling the acquisition of profile walls, can improve the results reasonably. Furthermore, the estimated parameter $\widehat{\gamma_{12}} = 0.9445$ is not significantly different from 1 indicating that the two root patterns are independent. Note that the interaction parameters γ_1 and γ_2 look similar, but since we chose different interaction radii, the strength of interaction differs, too. Therefore, there is no reason to simplify our model so that it has the same interaction parameter for each species.

Model validation. For the model validation (here goodness-of-fit testing), we compute the pointwise envelopes for the univariate L_{ii}-functions, $i = 1, 2$, of the homogenized data. The homogenization is done as in the case of the pair correlation function with respect to the vertical axis with the estimated parameters $\widehat{\eta}$, $\widehat{\alpha}$ and $\widehat{\beta}$ from Section 2 separately for *P. abies* and *F. sylvatica*.

First, we obtain estimates $\widehat{L_{11}(r)}$ and $\widehat{L_{22}(r)}$ as an average of those for each single homogenized point pattern. Then, we simulate the bivariate inhomogeneous saturation point process 7 times in W (because of 7 sampling windows) using the algorithm described in Section 5 and estimate the replicated L_{ii}-functions for this simulation run. From 200 simulation runs we compute pointwise envelopes. If the estimated functions are inside the corresponding envelopes, the model can be considered as appropriate. Fig. 7 shows the envelopes for the estimated $L_{ii}(r) - r$ functions of *P. abies* and *F. sylvatica*, respectively.

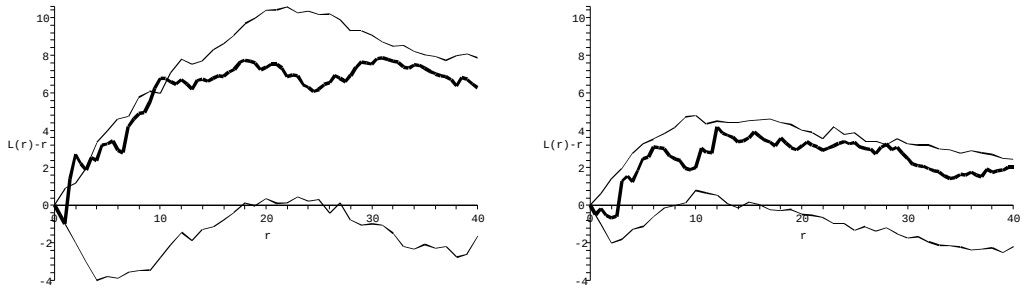

Fig. 7 Estimated mean univariate $L(r) - r$ functions for homogenized data of *P. abies* (left) and *F. sylvatica* (right) with pointwise 99% envelopes (shown by thin lines) of the fitted model

Note that it is not possible to use the L_{12}-function, since the vertical depth densities for *P. abies* and *F. sylvatica* differ and thus the homogenization approach is not applicable.

7 Discussion

A new approach of modelling and analyzing inhomogeneous replicated marked point patterns has been presented. We fitted a bivariate inhomogeneous saturation point process to the roots of *P. abies* and *F. sylvatica* in mixed stands. The novelty of this approach is the inclusion of the specific inhomogeneity which does not only appear in the density function of the bivariate inhomogeneous saturation point process, but is also reflected in the definition of the neighborhood, i.e. the influence region of the roots. Another challenge was the fitting of replicated point patterns, where we used the maximum pseudolikelihood method. Note that the presented approach can easily be extended to more than two types of roots.

For model validation we only considered a point process characteristic of the homogenized univariate point patterns. We computed envelopes for the estimated averaged L_{ii}-functions (Fig. 7). For *F. sylvatica* the chosen model seems to be a good fit, but for short distances the estimated L-function of *P. abies* hits the envelope. Nevertheless, altogether for both tree species, this simple model seems to be appropriate.

The estimated interaction parameters γ_1 and γ_2 seem to be quite similar, i.e. in mixed stands the roots of *P. abies* are clustered as strongly as the roots of *F. sylvatica*, but in a larger region. A further reduction of the model could be obtained by the assumption $\gamma_1 = \gamma_2$, which from a biological point of view is not reasonable. Moreover, our estimated interspecific interaction parameter $\widehat{\gamma_{12}}$ is not significantly different from 1, i.e. there is no clear evidence that interspecific interaction between roots of *P. abies* and roots of *F. sylvatica* occurs in the data set. Note that we used a model with only one cross-interaction parameter, γ_{12}. The model can be extended to have two parameters, γ_{12} for the type 1 affected by neighbor points of type 2 and γ_{21} for the type 2 affected by neighbor points of type 1. Allowing $\gamma_{12} \neq \gamma_{21}$ would then result in a model with non-symmetric cross-interaction - this is a feature which is not considered in Gibbs models literature so far. However, given the small number of roots in each point pattern, we have taken only one cross-interaction parameter in order not to increase the number of parameters too much.

The spatial distributions of roots of *P. abies* and *F. sylvatica* in pure stands have been modelled by inhomogeneous Matérn cluster point processes (Fleischer et al., 2006) and the roots of *P. abies* show stronger clustering in a smaller region of attraction than the roots of *F. sylvatica*. Our results suggest that the stronger clustering of roots of *P. abies* compared to roots of *F. sylvatica* in pure stands is also present in mixed stands. Note that although the estimates of the interaction parameters are close, the regions of attraction are not the same for the two species. The interaction distances were determined by means of the univariate pair correlation function and were fixed for the estimation of the other model parameters. A more profound discussion of the structural differences between the root distributions in pure and mixed

stands, respectively, could be done if the univariate inhomogeneous saturation point process would also be fitted to the root profile walls in pure stands, which is subject to future work.

Roots react to nutrient-enriched soil patches by enhanced growth and greater biomass in the areas, where the roots are clustered. Hodge (2004; 2006) and Kazda and Schmid (2008) discuss different reasons for the clustering of tree roots, which can be seen as an indication of extensive intraspecific competition. Indeed, Schmid and Kazda (2001) found about 25% higher growth rate of beech coarse roots ($> 5\ mm$) compared to spruce in mixed stands. The small roots investigated in this study were described with regard to water and nutrient uptake (Lindenmair et al., 2001) and they mediate to the most active fine roots. Thus, clusters of small roots reflect the presence of nutrient patches or zones of better water availability (Hodge, 2004; Parker and van Lear, 1996).

Schmid and Kazda (2005) found that the number of small roots and their clustering were independent of the distance to and the diameter of the surrounding trees. Root clustering is seen as a rule in natural soils for optimized exploitation of aggregated resources (Kazda and Schmid, 2008) but the interaction between roots of different species within such clusters was so far unknown. The present work suggests that there is no statistically significant interaction of roots of *P. abies* and *F. sylvatica* with respect to their spatial distribution. The approach introduced in this paper offers a possibility to deal with such intraspecific and interspecific interactions.

Acknowledgements We thank I. Schmid for her efforts in data acquisition. We are also greatful for the valuable comments made by the two referees and the associate editor. S. Eckel is supported by a grant of the graduate college 1100 at Ulm University. The work was partly made when P. Grabarnik was visiting the Institute of Stochastics, Ulm University, a hospitality of which he acknowledges very much. A. Särkkä has been supported by the Swedish Research Council and the Swedish Foundation for Strategic Research.

References

Baddeley, A. and van Lieshout, M. N. M (1995). Area-interaction point processes. *Annals of the Institute of Statistical Mathematics* **47**, 601-619.

Baddeley, A. and Turner, R. (2000). Practical maximum pseudolikelihood for spatial point patterns (with discussion). *Australian and New Zealand Journal of Statistics* **42**, 283-322.

Baddeley, A., Gregori, P., Mateu, J., Stoica R., and Stoyan, D. (eds.) (2006). Case studies in spatial point process modeling. *Lecture Notes in Statistics* **185**. Springer, New York.

Bell, M. L. and Grunwald, G. K. (2004). Mixed models for the analysis of replicated spatial point patterns. *Biostatistics* **5**, 663-648.

Berman, M. and Turner, R. (1992). Approximating point process likelihoods with GLIM. *Applied Statistics* **41**, 31-38.

Diggle, P., Fiksel, T., Grabarnik, G., Ogata, Y., Stoyan, D. and Tanemura, M. (1994). On parameter estimation for pairwise interaction processes. *International Statistical Review* **62**, 99-117.

Diggle, P. J., Mateau, J. and Clough, H. E. (2000). A comparison between parametric and nonparametric approaches to the analysis of replicated spatial point patterns. *Advances in Applied Probability* **32**, 331-343.

Diggle, P. (2003). *Statistical analysis of spatial point patterns* (2nd edition). Arnold, London.

Finkenstädt, B., Held, L. and Isham, V. (eds.) (2006). *Statistical methods for spatio-temporal systems.* Chapman & Hall, Boca Raton.

Fleischer, F., Eckel, S., Schmid, I., Schmidt, V. and Kazda, M. (2006). Point process modelling of root distributions in pure stands of Fagus sylvatica and Picea abies. *Canadian Journal of Forest Research* **36**, 227-237.

Geyer, C. J. and Møller, J. (1994). Simulation procedures and likelihood inference for spatial point processes. *Scandinavian Journal of Statistics* **21**, 359-373.

Geyer, C. J. (1999). Likelihood inference for spatial point processes. In: *Stochastic Geometry. Likelihood and Computation.* Barndorff-Nielsen, O. E., Kendall, W. S. and van Lieshout, M. N. M. (eds.). Chapman and Hall, London, 79-140.

Goulard, M., Särkkä, A. and Grabarnik, P. (1996). Parameter estimation for marked Gibbs point processes through the maximum pseudolikelihood method. *Scandinavian Journal of Statistics* **23**, 365-379.

Grabarnik, P. and Särkkä, A. (2001). Interacting neighbour point processes: some models for clustering. *Journal of Statistical Computation and Simulation* **68**, 103-126.

Grabarnik, P., Loic, P. and Bengough, G. (1998). Simulation study of the geometrical properties of a maize crop root system, and its consequences for root length density and root intersection density. *Plant and Soil* **200**, 157-167.

Hahn, U., Jensen, E. B. V., van Lieshout, M. N. M. and Nielsen, L. S. (2003). Inhomogeneous spatial point processes by location dependent scaling. *Advances in Applied Probability* **35**, 319-336.

Hahn, U., Micheletti, A., Pohlink, R., Stoyan, D. and Wendrock, H. (1999). Stereological analysis and modelling of gradient structures. *Journal of Microscopy* **195**, 113-124.

Hodge, A. (2004). The plastic plant: root responses to heterogeneous supplies of nutrients. *New Phytologist* **162**, 9-24.

Hodge, A. (2006). Plastic plants and patchy soils. *Journal of Experimental Botany* **57**, 401-441.

Illian, J., Penttinen, A., Stoyan, H. and Stoyan, D. (2008). *Statistical Analysis and Modelling of Spatial Point Patterns.* J. Wiley & Sons, Chichester.

Jackson, R. B. and Caldwell, M. M. (1996). Integrating resource heterogeneity and plant plasticity: modelling nitrate and phosphate uptake in a patchy soil environment. *Journal of Ecology* **84**, 891-903.

Jensen, E. B. V. and Nielson, L. S. (2000). Inhomogeneous Markov point processes by transformation. *Bernoulli* **6**, 761-782.

Kazda, M. and Schmid, I. (2008). Clustered distribution of tree roots and soil water exploitation. *Progress in Botany* **70**, 223-239.

Krasnoperov, R. A. and Stoyan, D. (2004). Second-order stereology of spatial fibre systems. *Journal of Microscopy* **216**, 156-164.

Lindenmair, J., Matzner, E., Göttlein, A., Kuhn, A. J. and Schröder, W. H. (2001). Ion exchange and water uptake of coarse roots of mature Norway spruce trees (*Picea abies* (L.) Karst.). In: *Plant Nutrition - Food Security and Sustainability of Agro-ecosystems*. Horst, W. J., Sattelmacher, B., Schmidhalter, U., Schubert, S., von Wiren, N., Wittenmayer, L., Schenk, M. K., Burkert, A., Claassen, N., Flessa, H. (eds.). Kluwer, Dordrecht, 568-569.

Mateu, J. (2001). Parametric procedures in the analysis of replicated pairwise interaction point patterns. *Biometrical Journal* **43**, 375-394.

Mayer, J., Schmidt, V. and Schweiggert, F. (2004). A unified simulation framework for spatial stochastic models. *Simulation Modelling Practice and Theory* **12**, 307-326.

Møller, J. (1999). Markov chain Monte Carlo and spatial point processes. In: *Stochastic Geometry. Likelihood and Computation*. Barndorff-Nielsen, O. E., Kendall, W. S. and van Lieshout, M. N. M. (eds.). Chapman & Hall, Boca Raton, 141-172.

Møller, J. and Waagepetersen, R. P. (2004). *Statistical inference and simulation for spatial point processes*. Chapman & Hall, New York.

Nielsen, L. S. and Jensen, E. B. V. (2004). Statistical inference for transformation inhomogeneous point processes. *Scandinavian Journal of Statistics* **31**, 131-142.

Ogata, Y. and Tanemura, M. (1986). Likelihood estimation of interaction potentials and external fields of inhomogeneous spatial point patterns. In: *Proceedings of the Pacific Statistical Congress 1985*. Francis, I. S., Manly, B. F. J and Lam, F. C. (eds.). Elsevier, Amsterdam, 150-154.

Parker, M. M. and van Lear, D. H. (1996). Soil heterogeneity and root distribution of mature loblolly pine stands in piedmont soils. *Soil Science Society of America Journal* **60**, 1920-1925.

R Development Core Team (2006). R: A language and environment for statistical computing. R Foundation for Statistical Computing, Vienna, Austria. ISBN 3-900051-07-0, URL http://www.R-project.org.

Ripley, B. D. (1977). Modelling spatial patterns (with discussion). *Journal of the Royal Statistical Society Series B* **39**, 172-212.

Robert, C. P. and Casella, G. (2004). *Monte Carlo statistical methods* (2nd edition). Springer, New York.

Schenk, H. J. (2005). Vertical vegetation structure below ground: scaling from root to globe. *Progress in Botany* **66**, 341-373.

Schmid, I. and Kazda, M. (2001). Vertical distribution and radial growth of coarse roots in pure and mixed stands of Fagus sylvatica and Picea abies. *Canadian Journal of Forest Research* **31**, 539-548.

Schmid, I. and Kazda, M. (2002). Root distribution of Norway spruce in monospecific and mixed stands on different soils. *Forest Ecology and Management* **159**, 37-47.

Schmid, I. and Kazda, M. (2005). Clustered root distribution in mature stands of Fagus sylvatica and Picea abies. *Oecologia* **144**, 25-31.

Stoyan, D. and Stoyan, H. (1998). Non-homogeneous Gibbs process models for forestry - a case study. *Biometrical Journal* **40**, 521-531.

Strauss, D. J. (1975). A model for clustering. *Biometrika* **52**, 1670-1684.